Monitoring dynamic concrete beam deformation with range cameras

Xiaojuan QI and Derek LICHTI, Canada

Key words: Range camera, deformation, structural measurement, dynamic deformation measurement

SUMMARY

The need to measure deformation in concrete beams, as integral components of bridges and other of structures, is well recognized due to the decaying state of civil infrastructure in Canada and in many other countries. Imaging techniques based on digital cameras, laser scanners and range cameras have been proven to be accurate and cost-effective methods for large-area measurement of deformation under static loading conditions. However, methods for the measurement of deformation under dynamic loading conditions are also necessary since knowledge about the behaviour of beams due to fatigue is critical for the assessment of safety. This paper presents a low-cost and high accuracy imaging technique to measure dynamic deformation in concrete beam with range cameras. A range camera is an ideal measurement device because of its ability to directly measure video sequences of three-dimensional co-ordinates of entire surfaces. However, due to the measurement principle of range cameras (i.e. four successive integration periods are required) target or sensor movement could lead to motion artefacts that degrade range measurement accuracy. It is demonstrated herein both by simulation and with real data that small amplitude (4 mm) and low frequency (1 Hz) target motion in fatigue load testing does not adversely affect deformation measurement. The results show that the 1 Hz periodic motion of the beam can be recovered from the time series with sub-millimetre accuracy when compared with laser displacement sensors.

Monitoring dynamic concrete beam deformation with range cameras

Xiaojuan QI and Derek LICHTI, Canada

1. INSTRUCTION

Concrete beams are integral components of bridges and other structures. Cracking due to overloading and corrosion of the reinforcing steel can be lead to degration of a beam's strength, so structural engineers and researchers have been investigating various reinforcement methods. For example, carbon fiber-reinforced polymer (FRP) composites have been investigated to strengthen existing older bridges and powder actuated fastening systems to attach the FRP strips to the concrete surface is presented by Lamanna et al. (2002). Concrete beam can be strengthened by the addition of steel plates. The efficacy of such methods can be evaluated through fatigue load testing in which cyclic loads are applied to a beam in a laboratory.

The objective of the current research is to measure the deformation of a concrete beam with carbon fibre-reinforced polymer composites subjected to periodic loads from a hydraulic actuator using range cameras in a lab.

Accurate concrete beam dynamic deformation monitoring can be performed with different sensors such as dial gauges, linear-variable differential transformers and laser displacement sensors (LDSs). Maas and Hampel (2006) reported that the sensors provide high geometric precision, accuracy and reliability for deformation measurement. However, the drawbacks are that they are point-wise devices and offer only one-dimensional measurement ability. If two- or three-dimensional measurements are required, those sensors could be useless.

Therefore, recently, a great deal of research has been concentrated on deformation measurement with photogrammetric methods in order to obtain a large-area and three-dimensional (3D) coverage. Photogrammetric methods comprise of terrestrial laser scanning (TLS), traditional photogrammetry with several regular cameras and range cameras (RCs). TLS was investigated to measure the deformation of the concrete beam by Gordon et al. (2007). However, TLS cannot be used to monitor the dynamic deformation of structures due to its sequential data collection. Traditional photogrammetry can be used to determine the dynamic deformation of the concrete beam but requires multiple synchronized and oriented images with overlapping fields of views. The RCs are an attractive choice for dynamic deformation monitoring for several reasons. First, a single RC can perform video rate 3D measurement of entire surfaces of extended structures such as concrete beams. Second, the

RCs are much more compact in size so that they can be mounted easily. Third, the cost of RCs is about an order of magnitude lower than a laser scanner.

This paper is structured as follows. Section 2 describes the measurement principle of the RCs and the effect of target motion on the ranges. Section 3 discusses the fatigue loading experiment conducted on a concrete beam. Section 4 gives the results from both simulations and the real experiment. Section 5 concludes the contribution of this research.

2. MEASUREMENT PRICIPLE

2.1 Range imaging measurement principle

Three-dimensional RCs are new generation of active cameras that operate by the time-of-flight principle. A cone of amplitude-modulated near-infrared light signals emitted from a set of integrated light emitting diodes on the camera illuminates the scene to be measured. The reflected light from the scene is focused by the lens onto a solid-state sensor. The received signal is demodulated at each pixel location from the measurements of the cross-correlation function from four successive integration periods (Equations 1-4) to determine the phase difference and thus, the range to the target surface as well as the amplitude of the received signal. For each integration period, the phase of the modulating envelope is shifted by 90°. A detailed description of this principle can be found in Lange and Seitz (2001).

$$C_0 = \frac{A}{2}\cos \emptyset + K \tag{1}$$

$$C_1 = -\frac{A}{2}\sin \emptyset + K \tag{2}$$

$$C_2 = -\frac{A}{2}\cos \emptyset + K \tag{3}$$

$$C_3 = \frac{A}{2}\sin \emptyset + K \tag{4}$$

where, A is the emitted signal amplitude and K is the offset added the model background illumination.

The phase difference between the received and emitted signals, $\emptyset$ is derived from a combination of the four measurements (Equation 5) and the range, ρ (Equation 6) is derived by scaling the phase difference.

$$\emptyset = \tan^{-1}\left(\frac{C_3 - C_1}{C_0 - C_2}\right) \tag{5}$$

$$\rho = \frac{\emptyset c}{4\pi f_m} \tag{6}$$

where, f_m is modulation frequency, c is the speed of light.

2.2 Effect of the target motion

The range imaging measurement principle assumes that the object is stationary during the four integration periods. However, when the target or the RCs is moving during the four integration times, each measurement (Equations 1-4) will contain an additional time-dependent phase shift, $\Delta\emptyset_i$ showed in (Equation 7) that will cause the phase difference to be biased.

$$\widehat{C_i} = \frac{A}{2}\cos(\emptyset + \frac{\pi i}{2} + \Delta\emptyset_i) + K \tag{7}$$

If the target motion is a sinusoid, as is the case in fatigue load testing, and the range camera is oriented such that the motion is confined to the radial direction, the periodic change in range is given by Equation (8). Therefore the additional phase shift is Equation (9):

$$\Delta\rho(t) = a\sin(2\pi f_0 t) \tag{8}$$

$$\Delta\emptyset(t) = \frac{4\pi f_m}{c}\Delta\rho(t) \tag{9}$$

where a is the amplitude of the target motion; f_0 is the frequency of the target motion.

Using the Equations (8 and 9), the sampling measurement i is thus given by Equation (10).

$$\widehat{C_i} = \frac{A}{2}\cos(\emptyset + \frac{\pi i}{2} + \frac{4\pi f_m}{c}\, a\sin(2\pi f_0 t)) + K \tag{10}$$

With the biased sampling measurement, the biased phase difference (Equation 11) is derived.

$$\widehat{\emptyset} = \tan^{-1}\left(\frac{\widehat{C_3}-\widehat{C_1}}{\widehat{C_0}-\widehat{C_2}}\right) \tag{11}$$

The impacts of the target motion on the range measurements are assessed in Section 4.1.

2.3 Deformation measurement from range cameras

The 3D co-ordinates (X_i, Y_i, Z_i) of a point observed by a range camera can be determined by scaling the image point vector by the range, ρ_i with Equation 12 (Lichti et al., In press).

$$\begin{bmatrix} X_i \\ Y_i \\ Z_i \end{bmatrix} = \frac{\rho_i}{\sqrt{(x_i)^2+(y_i)^2+{p_d}^2}} \begin{bmatrix} x_i \\ y_i \\ -p_d \end{bmatrix} \tag{12}$$

where, p_d is the principal distance of the range camera; (x_i, y_i) are the target image co-ordinates corrected for systematic errors; ρ_i is the range measurement corrected range errors.

The measurement of beam deformation, the target application described in this paper, can be made from a nadir-looking range camera. The depth (Z) of the target is used to calculate the deformation of the beam (Lichti et al., In press).

3. EXPERIMENT DESCRIPTION

3.1 The measurement system to the dynamic concrete beam deformation

The measurement subject is a 3 m long, white-washed reinforced concrete beam having a 150 mm x 300 mm rectangular cross section. A hydraulic-actuator was used to apply the periodically-varying loads to the concrete beam through a spreader beam in contact with the top surface of the concrete beam. The system for measuring the dynamic concrete beam deformation comprised a target system and the measurement devices.

Since most of the top surface of the concrete beam was occluded by the spreader beam, the target system comprised thirteen white-washed, thin aluminum plates (220 mm x 50 mm) were to the side of the beam at an interval of 250 mm along its length. Two measurement devices were used: two SwissRanger SR4000 range cameras and several laser displacement sensors.

The pixel array size of the SR4000 is 176 × 144 and it has a pixel pitch of 40 μm with a 5.8 mm focal-length lens. It has a non-ambiguity range of 5 m with the default modulation frequency of 30 MHz, though this parameter can be set by the user to one of values (29, 30 and 31 MHz). The measurement absolute accuracy of the range cameras is ±10 mm provided by the manufacturer. For more details about the SR4000 range camera, see the SR4000 Manual (2009). The two SR4000 range cameras were positioned on either side of the hydraulic actuator with be nadir-looking orientation and 1.9 m standoff distance for complete coverage of the beam.

The deformation measurements were also recorded by five vertically-oriented KEYENCE LKG407 CCD laser displacement sensors positioned directly under the centroid of five of the aluminum plates. This device measures displacement by active laser triangulation. The manufacturer's stated linearity and precision for this transducer are 0.05% of the ±100 mm measurement range and 2 μm, respectively. Therefore, the LDSs were used as a benchmark for assessing the accuracy of the beam deformation measurement with the range cameras.

Figure 1a illustrates the experiment setup for a dynamic deformation experiment which was conducted in the Structural Laboratory at the University of Calgary. Figure 1b shows the LDSs for monitoring the thin plate which is a part of Figure 1a.

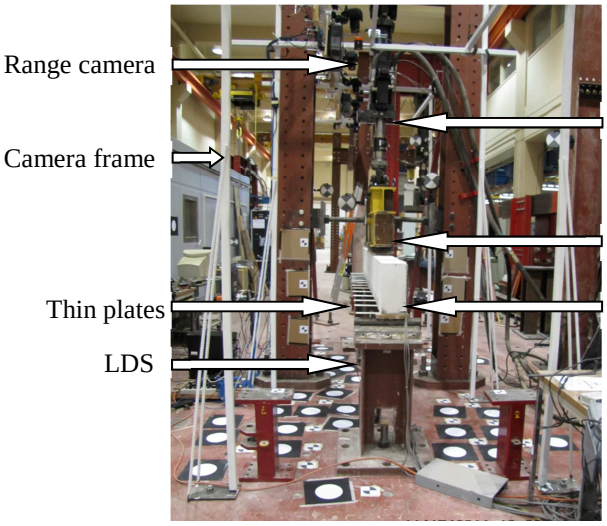

Figure 1a The experiment setup for a dynamic deformation experiment

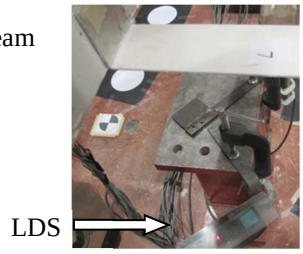

Figure 1b The LDS for monitoring the thin plate

3.2 Loading procedure and data capture

Before the dynamic loading test was performed, a static loading regime based on displacement control and load control was executed in four steps. First, the static loading was based on displacement control by applying a displacement of 3 mm at a rate of 1 mm/min. Second, the concrete beam was unloaded to zero displacement at the same rate of 1mm/min. Third, a displacement of 3 mm was applied at the same rate. Fourth, the concrete beam was applied to zero displacement at the same rate. Next load-control loading was executed. A load of 24 kN at a rate of 6 kN/min was applied twice to the beam. After this, the dynamic loading with 4 mm amplitude (8 mm peak-to-peak displacement) was then conducted at a loading frequency 1Hz. Over 10000 load cycles were applied from 24 kN to 96 kN.

Several factors required attention for the data capture. First, the 3D range cameras had to be warmed up for one hour to obtain stable measurement data. Second, the illumination of the two cameras would interfere with each other if they were operated with the same modulation frequency. Two different modulation frequencies (29 MHz and 31 MHz) were therefore used to prevent light interference. In addition, the integration times for both were set at 21 ms, for which the corresponding frame sampling frequency is 10 Hz, which clearly exceeds the minimum rate of 2 Hz required to sample the 1 Hz motion. It is also important to note that range measurements to the thin plates were biased by range scattering error (Jamtsho and

Lichti, 2010). Since, however, only the relative, periodic motion is desired, the range bias due to scattering at each target location is of no consequence.

3.3 Data processing

Despite the simplicity of the range camera image acquisition, the automatic extraction of the objects of interest, namely the thin plates bonded to the beam from the RC data requires specialised image processing techniques. Since an RC simultaneously produces a co-located range and amplitude images, both radiometric and depth information can be used to segment the thin plates. The thin plate extraction process is briefly described as follows. First, depth-based classification is used to remove the floor and the upper of the thin plates such as hydraulic actuator, spreader beam and top surface in the amplitude image (Figure 2). Second, a binary image is determined from the amplitude image with the image threshold estimated by the Otsu method (Otsu, 1979). Third, eccentricity is used to classify the thin plates because the eccentricity of the bar-like regions is similar throughout the image (Rohs, 2005). Fourth, the boundaries were removed with image erosion algorithm because the mixed pixels occur frequently at the edges. Figure 3 illustrates the final result of the thin plate segmentation.

Figure 2 The gray scale image of the deformation scene

Figure 3 The final result of the thin segmentation

4. RESULTS AND ANALYSIS

4.1 Analysis to affect of target motion

Motion artefacts occur as a result of target or sensor motion during data capture due to the range camera measurement principle. Ideally the trajectory of the thin plate centroid motion is a sinusoidal curve. Therefore, a simulation study has been conducted to examine the effects of sinusoidal motion in this work. In this section, a target experiencing sinusoidal motion with the frequency of 1 Hz and 4 mm amplitude was simulated. The frame sampling frequency was set at 10 Hz. Figure 4 illustrates the true and biased periodic ranges to the moving target. As

can be seen, the amplitude difference between them is small but there is a phase difference. The phase difference is -13.2° but it is of no consequence since it does not affect the amplitude measurement accuracy. So, the phase difference prime importance. Figure 5a shows the magnitude spectrum of the true target motion and Figure 5b shows the magnitude spectrum of the biased target motion. The difference between magnitudes is only -0.061 mm, which is 1.5% of the amplitude 4 mm.

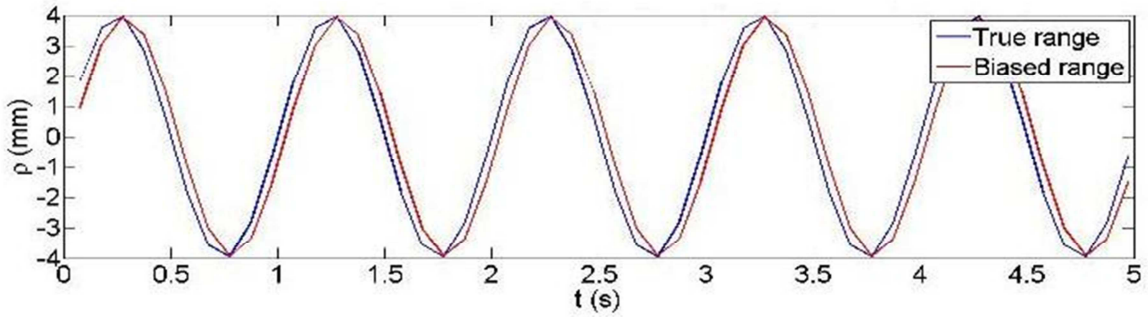

Figure 4 The periodic range to the moving target

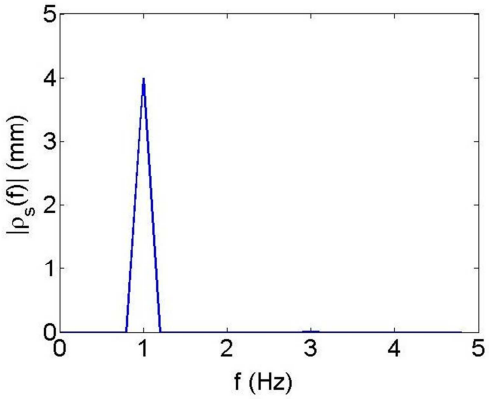

Figure 5a The magnitude spectrum analysis of the true target motion

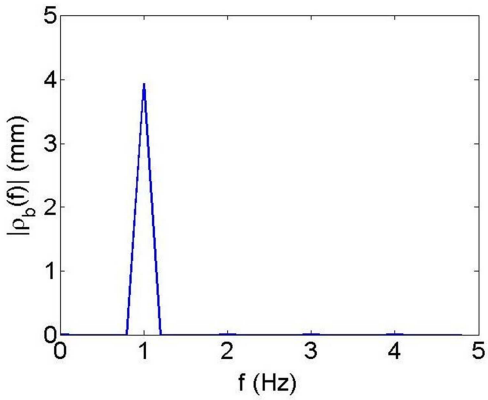

Figure 5b The magnitude spectrum analysis of the biased target motion

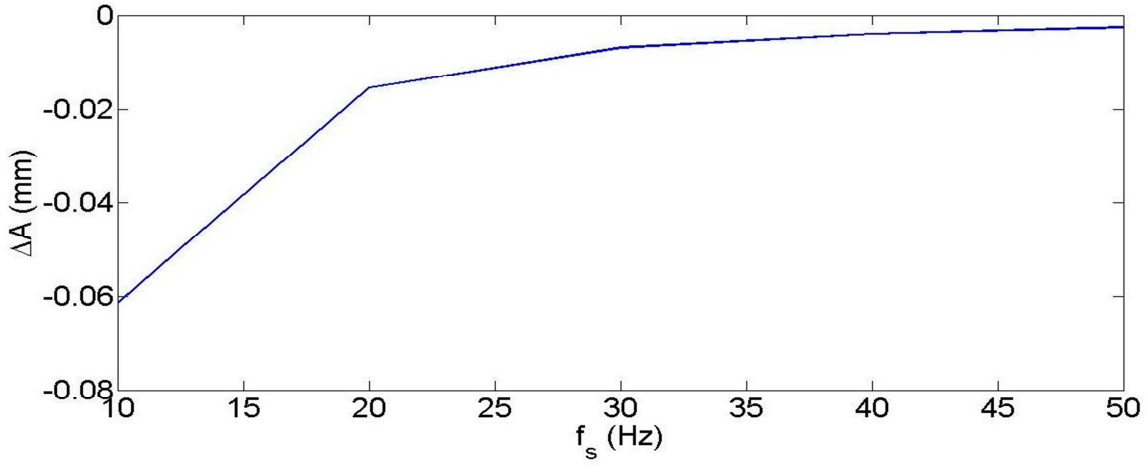

Figure 6 The sinusoidal amplitude differences

Figure 6 shows the amplitude difference between the true and estimated signals as a function of the frame sampling rate f_s. As can be seen, increasing the sampling frequency results in a reduction of the amplitude error. In the beam deformation measurement experiment, the sampling frequency was 10 Hz and the loading frequency was 1 Hz. As a result, it is expected that the motion artefact does not affect the deformation measurement reliability when the maximum amplitude of the periodic sinusoidal load is 4 mm.

4.2 Trajectory analysis of the thin plate and the deformation of the concrete beam

Absolute evaluation of the motion trajectory of the thin plate and the deformation of the concrete beam with the range cameras was performed by comparing the motion trajectory and deformation estimated from the range cameras and the independent measurement with LDSs at the same time. The maximum deformation can be measured by tracking the centroid of a thin plate located close to the mid-span of the beam with an LDS using 300 Hz sampling frequency. One of the thirteen plates located close to the mid-spin of the concrete beam was selected.

In the beam deformation experiment, the motion of the thin plate centroid is ideally a sinusoidal waveform. The sinusoidal waveform can be analyzed easily in frequency domain from which the signal frequency and amplitude can be derived. Therefore, spectral analysis methods were used to analyze the thin plate centroid data. Although, the range camera time series was uniformly sampled at 10 Hz, some random drop-outs occurred, which is called the missing data problem. Since uniformly-sampled data could not be obtained, conventional spectral analyses of the thin plate centroid Z data could be performed. Instead, spectral analysis of the unevenly sampled data was conducted with the Lomb method (Press et al., 1992). Figure 7 shows the so-obtained power spectrum of the thin plate centroid measured

with one of the range cameras. As can be seen, there is one dominant peak in the spectrum at the loading frequency. The loading frequency was estimated by the thin plate spectral analysis to be 1.0286 Hz. The thin plate centroid depth data from LDSs were analyzed with the same procedure. Figure 8 shows the so-obtained power spectrum of the same thin plate measured with one of the LDSs. As we can see, there is one dominant peak in the spectrum at the loading frequency which was estimated to be 1.0296 Hz. Thus, the loading frequency difference was obtained with RC and LDS is 0.001 Hz which is not a significant.

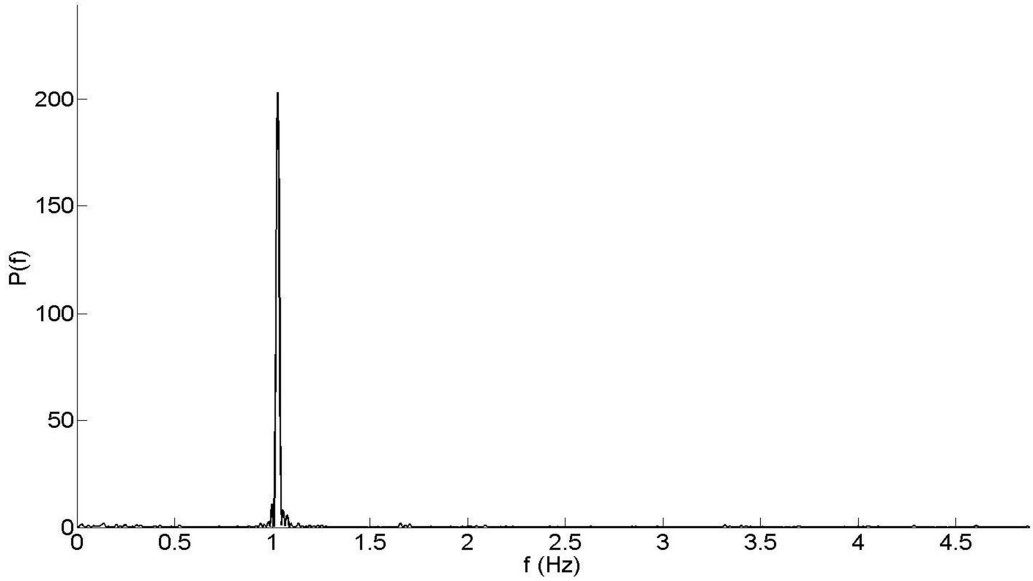

Figure 7 The spectral analysis of the thin plate centroids from the RC

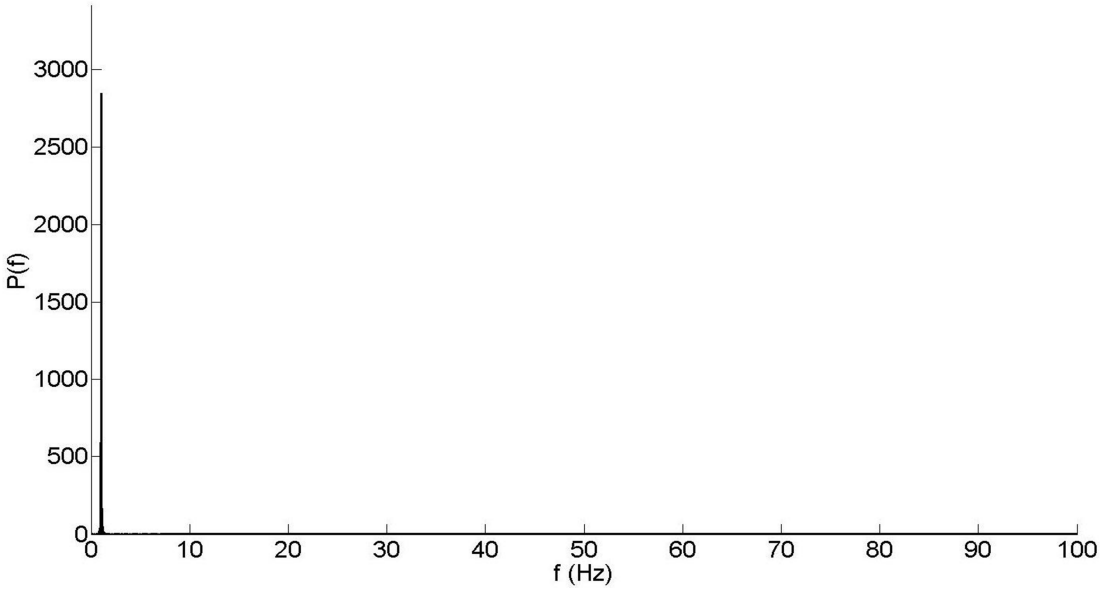

Figure 8 The spectral analysis of the thin plate centroids from the LDS

With the recovered loading frequency, the amplitude of the thin plate trajectory was estimated by the harmonic model (Equation 13) using least-squares. Figure 9 illustrates the trajectories of the chosen thin plate estimated from the RC and LDS data. As can be seen, the estimated trajectories matched very well. The estimated amplitude of the thin plate motion measured with the RC is 3.6 mm and is 3.9 mm from the LDS. The amplitude difference between the RC and LDS is only 0.3 mm. Therefore, the maximum deformation difference of the concrete beam is 0.3 mm by comparing the RC and LDS measurement. The absolute accuracy of the beam deformation with the RC is smaller than the ±10 mm absolute accuracy reported by the manufacturer.

$$h(t) = A\cos 2\pi f_0 t + B\sin 2\pi f_0 t \tag{13}$$

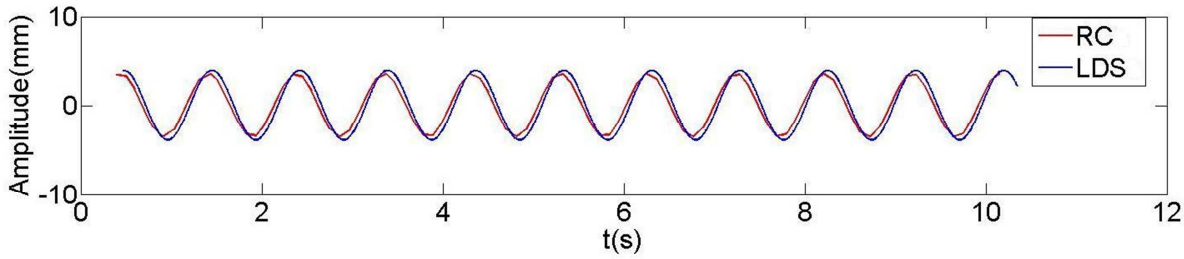

Figure 9 The estimated trajectories of the one thin plate centroid from the RC and LDS

5. CONCLUSIONS

The deformation measurement of a concrete beam subjected to the periodic loading has been made with sub-millimetre accuracy using a range camera. The paper has shown by simulation that artefacts due to the nature of the RC measurement and target motion do not adversely affect the deformation measurement reliability when the periodic sinusoidal motion has 4 mm amplitude and 1 Hz frequency. The results from real data have indicated that periodic deformation can be recovered with sub-millimetre accuracy when the 1 Hz target motion is sampled at 10 Hz.

ACKNOWLEDGEMENTS

Funding for this research was provided by the Natural Sciences and Engineering Research Council of Canada (NSERC) and the Canada Foundation for Innovation (CFI).

REFERENCES

Elrefai, A. West, J and Soudki, K., (2008), Effect of overloading on fatigue performance of reinforced concrete beams strengthened with externally post-tensioned carbon-fibre-reinforced polymer tendons, *Canadian Journal of Civil Engineering*, Vol. 35, pp 1294-1307.

Gordon, S., Lichti, D., Franke, J., and Stewart, M., (2007), Modeling terrestrial laser scanner data for precise structural deformation measurement, *ASCE Journal of Surveying Engineering*, Vol. 133, pp 72-80.

Jamtsho, S. and Lichti, D.D., (2010), Modeling scattering distortion of 3D range camera, *The International Archives of the Photogrammetry, Remote Sensing and Spatial Information Sciences*, Newcastle upon Tyne, UK, Vol. XXXVIII, pp 299-304.

Lamanna, A.J., Bank, L.C., Borowicz, D.T., and Arora, D., (2002). Strengthening of concrete beams with mechanically fastened FRP strips, *Third International Conference on Composites in Infrastructure,* San Francisco, USA.

Lange, R. and Seitz, P., (2001), Solid-state time-of-flight range camera, *IEEE Journal of Quantum Electronics*, Vol. 37, pp 390-397.

Lichti, D.D., Jamtsho, S., El-Halawany, I. S., Lahamy, H., Chow, J. Chang, T. O. and El-Badry, M., Structural deflection measurement with a range camera, *Journal of Surveying Engineering*, In press.

Lindner, M. and Kolb, A., (2009), Compensation of motion artifacts for time-of-flight cameras, *Dyn3D, LNCS 5742*, Vol. 5742, pp 16-27.

Maas, H., and Hampel, U., (2006), Photogrammetric techniques in civil engineering material testing and structure monitoring, *Photogrammetric Engineering & Remote Sensing*, Vol. 72, pp 39-45.

Otsu, N., (1979), A threshold selection method from gray-level histograms, *IEEE Transactions on Systems, Man, and Cybernetics*, Vol. 9, pp 62-66.

Press, H., W., Teukolsky, A., S., Vetterling, T., W., and Flannery, P., B., (1992), Numerical recipes in C, Second Edition, Cambridge University Press, pp 575-581.

Rohs, M., (2005), Real-world interaction with camera phones, *Lecture Notes in Computer Science*, Vol. 3598, pp 74-89.

SR4000 user manual, www.mesa-imaging.ch.

BIOGRAPHICAL NOTES

Xiaojuan Qi is currently a full-time graduate student in Department of Geomatics Engineering, University of Calgary, Canada. Her research topic is focusing on the dynamic deformation measurement of the concrete beam with range cameras.

Dr. Derek Lichti is currently Associate Professor in the Department of Geomatics Engineering at the University of Calgary, Canada, and Chair (2008-2012) of the International Society for Photogrammetry and Remote Sensing (ISPRS) Working Group V/3 Terrestrial Laser Scanning and 3D Imaging. His research activities focus on the modeling and use of optical and range imaging sensors for automated 3D object reconstruction for a broad spectrum of applications including structural measurement, mobile mapping and human-computer interaction.

CONTACTS

Xiaojuan Qi
Department of Geomatics Engineering
Schulich School of Engineering, University of Calgary
2500 University Drive N.W.
Calgary, Alberta, T2N 1N4
Canada
Tel. +1 (403) 220-4370
Fax + 1 (403) 284-1980
Email: xiqi@ucalgary.ca

Dr. Derek Lichti
Department of Geomatics Engineering
Schulich School of Engineering, University of Calgary
2500 University Drive N.W.
Calgary, Alberta, T2N 1N4
Canada
Tel. +1 (403) 210-9495
Fax + 1 (403) 284-1980
Email: ddlichti@ucalgary.ca